Angular Momentum Injection into a Penning-Malmberg Trap

Richard Fitzpatrick & Edmund P. Yu

Department of Physics & Institute for Fusion Studies, University of Texas at Austin, Austin TX

December 1995, Revised December 1996

Abstract

It is demonstrated using conventional fluid theory that angular momentum can be injected into a single component plasma confined in a Penning-Malmberg trap via an externally generated, oscillating, non-axisymmetric, electric field. The torque exerted on the plasma by the electric field is a highly non-monotonic function of the plasma angular rotation velocity. The torque *vs.* angular velocity curve is dominated by sharp resonances at which the angular phase velocity of a particular poloidal harmonic of the external field matches the plasma angular rotation velocity. The torque exerted on the plasma by a given poloidal harmonic is negative when the field rotates faster than the plasma, and *vice versa*. This rather surprising behaviour is shown to be entirely consistent with a standard result in hydrodynamic theory, but is generally not observed in present day experiments.

PACS: 52.25.Wz

I Introduction

Experiments involving single component plasmas confined in Penning-Malmberg traps are used extensively to investigate fundamental issues in fluid mechanics and plasma physics.[1−6] Single component plasmas possess the unique property that they can relax to thermal equilibrium without the loss of confinement.[7] In principle, a single component plasma can be confined in a Penning-Malmberg trap for an indefinite period of time. In practice, the confinement time is limited by small asymmetries in the externally generated magnetic field required to maintain the plasma equilibrium. Recently, "infinitely" long confinement of pure ion plasmas has been achieved by injecting momentum into the plasma using a rotating, non-axisymmetric, electric field.[8] The purpose of this paper is to investigate this phenomenon using conventional fluid theory.

II Analysis

A Basic scenario

Consider a cylindrical plasma of radius a made up of identical particles of charge q and mass M. The plasma is placed in a uniform axial magnetic field, of strength B_z, and surrounded by a vacuum region. This configuration is known as a *Penning-Malmberg trap*.

B Fundamental equations

The force balance equation for a cold (*i.e.*, zero pressure) single component plasma is

$$\frac{\partial \boldsymbol{v}}{\partial t} + (\boldsymbol{v}\cdot\nabla)\boldsymbol{v} = \frac{q}{M}(\boldsymbol{E} + \boldsymbol{v}\wedge\boldsymbol{B}) + \nu\left[\nabla^2\boldsymbol{v} + \frac{1}{3}\nabla(\nabla\cdot\boldsymbol{v})\right] - \gamma_d\,\boldsymbol{v}. \qquad (1)$$

Here, $\boldsymbol{v}$ is the fluid velocity, $\boldsymbol{E}$ the electric field, and $\boldsymbol{B}$ the magnetic field. The last two terms on the right hand side of the above equation are phenomenological. The former represents the diffusive transport of momentum throughout the

plasma; *i.e.*, viscosity. Experimentally, there is no doubt that a single component plasma possesses "viscosity" of some description, but its origins and nature are obscure.[9] A conventional electron-ion plasma possesses viscosity by virtue of collisions between particles.[10] Admittedly, this "collisional viscosity" is generally much smaller than the "anomalous viscosity" produced by fine scale turbulence (*i.e.*, collective effects).[11] A single component plasma also possesses a collisional viscosity.[12] However, the experimental viscosity exceeds this by several orders of magnitude.[9] The most likely explanation for the anomalous viscosity of a single component plasma is that it is also due to collective effects.[13] It remains unclear whether the observed "viscosity" of a non-neutral plasma is local (*i.e.*, diffusive) in nature, as is assumed in this paper for the sake of simplicity, or is a more complicated non-local effect.[14] The final term on the right hand side of Eq. (1) represents a gradual loss of plasma angular momentum due to small asymmetries in the magnetic field. It is well established experimentally that a single component plasma confined in a Penning-Malmberg trap eventually spins down because of non-uniformities in the axial magnetic field, but the exact nature of the angular momentum loss mechanism is unknown.[15] The clearest analogy in conventional plasma physics is "poloidal flow damping" in tokamaks.[16] In this phenomenon, the inevitable small variation of the toroidal magnetic field strength across the plasma due to the toroidal geometry interacts with *parallel* (to the magnetic field) plasma viscosity to produce a loss of angular momentum about the magnetic axis. The effective damping force exerted within the plasma is proportional to the local circulation velocity. This form for the damping force is adopted in Eq. (1). The coefficient of kinematic viscosity, ν, and the flow damping rate, γ_d, are both assumed to be constant across the plasma, for the sake of simplicity. Strictly speaking, it is the coefficient of dynamic viscosity $\mu = M n \nu$ which is constant in Eq. (1), which implies that $\nu \propto n^{-1}$. However, this paper is only concerned with plasmas whose density is uniform to lowest order. In this situation, it is consistent to neglect the variation of ν with density.

The continuity equation for a single component plasma is written

$$\frac{\partial n}{\partial t} + \boldsymbol{v}\cdot\nabla n + n\,\nabla\cdot\boldsymbol{v} = 0, \tag{2}$$

where n is the number density of particles.

Maxwell's equations for a non-relativistic single component plasma take the

form:

$$\nabla\cdot\boldsymbol{E} = \frac{nq}{\epsilon_0}, \tag{3a}$$

$$\nabla\cdot\boldsymbol{B} = 0, \tag{3b}$$

$$\nabla\wedge\boldsymbol{E} = -\frac{\partial\boldsymbol{B}}{\partial t}, \tag{3c}$$

$$\nabla\wedge\boldsymbol{B} = \mu_0 nq\,\boldsymbol{v}. \tag{3d}$$

According to Eqs. (1) and (3), the inductive component of the electric field and the modifications to the magnetic field due to plasma currents can both be neglected, since they are $O(v/c)^2$ smaller than the non-inductive electric field and the externally generated magnetic field, respectively. Thus,

$$\boldsymbol{E} = -\nabla\phi, \tag{4a}$$

$$\boldsymbol{B} = B_z\,\hat{\boldsymbol{z}}, \tag{4b}$$

where B_z is (approximately) constant. Note that B_z cannot be exactly constant, otherwise γ_d would be zero. However, in most Penning-Malmberg trap experiments the variations in B_z across the plasma are extremely small.[17] Equation (1) reduces to

$$\frac{\partial\boldsymbol{v}}{\partial t} + (\boldsymbol{v}\cdot\nabla)\boldsymbol{v} = \frac{q}{M}\left(-\nabla\phi + \boldsymbol{v}\wedge\hat{\boldsymbol{z}}\,B_z\right) + \nu\left[\nabla^2\boldsymbol{v} + \frac{1}{3}\nabla(\nabla\cdot\boldsymbol{v})\right] - \gamma_d\,\boldsymbol{v}, \tag{5}$$

and Eq. (3)(a) yields

$$\nabla^2\phi = -\frac{nq}{\epsilon_0}. \tag{6}$$

Conventional right handed cylindrical polar coordinates (r, θ, z) are adopted. For the sake of simplicity, the flow is assumed to be strictly two-dimensional:

$$\frac{\partial}{\partial z} = 0, \tag{7a}$$

$$v_z = 0. \tag{7b}$$

C Derived equations

Let

$$\boldsymbol{\omega} = \nabla \wedge \boldsymbol{v}, \tag{8a}$$

$$\zeta = \nabla \cdot \boldsymbol{v}, \tag{8b}$$

Equations (2), (5), (6), (7), and (8) yield

$$\frac{dn}{dt} = -n\,\zeta, \tag{9a}$$

$$\frac{d\omega_z}{dt} = -\omega_z\,\zeta - \Omega_c\,\zeta + \nu\,\nabla^2\omega_z - \gamma_d\,\omega_z, \tag{9b}$$

$$\frac{d\zeta}{dt} = -\nabla^2(v^2/2) + \boldsymbol{v}\cdot\nabla^2\boldsymbol{v} + {\omega_z}^2 + \frac{{\Omega_c}^2}{2}\frac{n}{n_c} + \Omega_c\,\omega_z + \frac{4\nu}{3}\nabla^2\zeta - \gamma_d\,\zeta, \tag{9c}$$

where

$$\frac{d}{dt} = \frac{\partial}{\partial t} + \boldsymbol{v}\cdot\nabla \tag{10}$$

is the total time derivative,

$$\Omega_c = \frac{qB_z}{M} \tag{11}$$

is the cyclotron frequency, and

$$n_c = \frac{{B_z}^2}{2\mu_0 M c^2} \tag{12}$$

is termed the *Brillouin density*.[18]

D Rigid rotator states

Plasma viscosity has the effect of relaxing the velocity profile of the plasma to that of a rigid rotator (assuming that the Debye length is small compared to

the plasma minor radius).[12] A rigidly rotating plasma possesses uniform density, vorticity, and divergence of the flow. In other words,

$$n(r,\theta,t) = n(t), \tag{13a}$$

$$\omega_z(r,\theta,t) = \omega_z(t), \tag{13b}$$

$$\zeta(r,\theta,t) = \zeta(t). \tag{13c}$$

The associated plasma velocity profile is given by

$$\boldsymbol{v} = \frac{1}{2}\left(r\zeta\,\hat{\boldsymbol{r}} + r\omega_z\,\hat{\boldsymbol{\theta}}\right). \tag{14}$$

The relationship between the plasma minor radius and the plasma density is

$$n\,a^2 = \text{constant}, \tag{15}$$

assuming that the plasma contains a fixed number of particles.

Substitution of Eqs. (13) and (14) into Eqs. (9) yields

$$\kappa\,\frac{\partial\Omega_\theta}{\partial t} \simeq -\gamma_d\,\Omega_\theta, \tag{16}$$

and

$$\bar{\Omega}_\theta{}^2 - \bar{\Omega}_\theta + \frac{\bar{n}}{4} \simeq 0, \tag{17}$$

where $\Omega_\theta = \omega_z/2$ is the uniform angular velocity of the plasma,

$$\bar{\Omega}_\theta = -\frac{\Omega_\theta}{\Omega_c} \tag{18}$$

is the normalized angular velocity,

$$\bar{n} = \frac{n}{n_c} \tag{19}$$

is the normalized plasma density, and

$$\kappa = \frac{1-\bar{n}/2}{\bar{n}/2}. \tag{20}$$

Equations (16) and (17) are only valid in the limit in which the flow damping rate is much less than the cyclotron frequency; *i.e.,* when $\gamma_d \ll |\Omega_c|$. This is certainly the case in all conventional Penning-Malmberg trap experiments.[9]

Equation (17) can be solved to give

$$\bar{\Omega}_\theta \simeq \frac{1}{2} \pm \frac{1}{2}\sqrt{1-\bar{n}}. \tag{21}$$

There are two branches of solutions. The plasma density increases with increasing angular velocity on the lower branch, but decreases with increasing angular velocity on the upper branch. In the former case the plasma is compressed by the $\boldsymbol{j} \wedge \boldsymbol{B}$ forces associated with the plasma rotation, in the latter case this effect is counteracted by the centrifugal force. The plasma attains its maximum density (the Brillouin density) when it rotates at half the cyclotron frequency. The plasma disperses as its angular rotation frequency either becomes much less than the cyclotron frequency or approaches the cyclotron frequency. Note that it is only possible to find rigid rotator equilibria for $\bar{n} \leq 1$ and $0 < \bar{\Omega}_\theta < 1$.

In the absence of any plasma angular momentum loss due to asymmetries in the axial magnetic field (*i.e.,* $\gamma_d = 0$) a rigid rotator state can, in principle, persist for an indefinite period of time. However, a non-zero momentum loss rate (*i.e.,* $\gamma_d > 0$) causes the plasma to slowly spin down. (Note that the factor κ in Eq. (16) is always positive.) Unless counteracted, this effect leads inevitably to the loss of plasma confinement since, according to Eqs. (15) and (21), once the plasma angular velocity falls below half the cyclotron frequency the plasma expands as it spins down.

E Angular momentum injection

Suppose that the plasma is perturbed in such a manner that its velocity field can be written

$$\boldsymbol{v}(r,\theta,t) = \boldsymbol{v}(r,t) + \tilde{\boldsymbol{v}}(r,t)\exp(\,\mathrm{i}\,m\theta), \tag{22}$$

where $|\tilde{\boldsymbol{v}}| \ll |\boldsymbol{v}|$. Operating on the θ-component of Eq. (5) with $\oint(\cdots)\, r^2\, d\theta/2\pi$ yields

$$\begin{aligned} r^3\,\frac{\partial\Omega_\theta}{\partial t} + r\,v_r\,\frac{\partial(r^2\,\Omega_\theta)}{\partial r} + \Omega_c\,r^2 v_r \quad &= \quad -\frac{1}{4}\frac{\partial}{\partial r}\left[r^2(\tilde{v}_r\,\tilde{v}_\theta^* + \tilde{v}_\theta\,\tilde{v}_r^*)\right] \\ &\quad + \frac{r^2}{4}(\tilde{v}_\theta\,\nabla\cdot\tilde{\boldsymbol{v}}^* + \tilde{v}_\theta^*\,\nabla\cdot\tilde{\boldsymbol{v}}) \\ &\quad + \nu\,\frac{\partial}{\partial r}\left(r^3\,\frac{\partial\Omega_\theta}{\partial r}\right) - \gamma_d\,r^3\,\Omega_\theta, \end{aligned} \tag{23}$$

where

$$\Omega_\theta(r,t) = \frac{v_\theta(r,t)}{r} \tag{24}$$

is the θ-averaged angular velocity profile of the plasma. Note that all terms which are linear in perturbed quantities average out of Eq. (23).

Assuming that the equilibrium state is one of the rigid rotator states described in Section II.D, and that the angular velocity of the plasma changes at a rate which is much less than the cyclotron frequency, Eq. (23) can be integrated across the plasma to give

$$\kappa\,\frac{\partial\Omega_\theta}{\partial t} \simeq \frac{4}{a^4}\int_0^a t_\theta(r)\,dr - \gamma_d\,\Omega_\theta, \tag{25}$$

where

$$t_\theta(r) = -\frac{1}{4}\frac{\partial}{\partial r}\left[r^2(\tilde{v}_r\,\tilde{v}_\theta^* + \tilde{v}_\theta\,\tilde{v}_r^*)\right] + \frac{r^2}{4}(\tilde{v}_\theta\,\nabla\cdot\tilde{\boldsymbol{v}}^* + \tilde{v}_\theta^*\,\nabla\cdot\tilde{\boldsymbol{v}}). \tag{26}$$

Equation (25) is clearly a generalization of Eq. (16). The new term on the right hand side represents the rate of angular momentum injection into the plasma via external perturbations. In the presence of such perturbations it is clearly possible for the plasma to achieve a steady state in which the rate of momentum injection matches the rate at which angular momentum is lost due to asymmetries in the axial magnetic field. In this situation, plasma confinement could, in principle, be maintained for an indefinite period of time, in spite of the effect of magnetic field asymmetries.

F Linear analysis

Suppose that the plasma has achieved a steady state with the aid of momentum injection from an external perturbation with m periods in the θ direction, oscillating at some angular frequency Ω. It follows that the plasma velocity can be written

$$\boldsymbol{v}(r,\theta,t) = r\,\Omega_\theta\,\hat{\boldsymbol{\theta}} + \tilde{\boldsymbol{v}}(r)\exp[\,\mathrm{i}\,(m\theta - \Omega t)]. \tag{27}$$

Likewise, the plasma density takes the form

$$n(r,\theta,t) = n + \frac{n_c}{\Omega_c}\,\tilde{n}(r)\exp[\,\mathrm{i}\,(m\theta - \Omega t)]. \tag{28}$$

Assuming that the perturbation is relatively small, linearization of Eqs. (9) yields

$$\alpha\,\bar{\Omega}_\theta\,\tilde{n} + \bar{n}\,\tilde{\zeta} = 0, \tag{29a}$$

$$(\bar{\gamma}_d + \alpha\,\bar{\Omega}_\theta)\,\tilde{\omega}_z + (1 - 2\bar{\Omega}_\theta)\,\tilde{\zeta} = \hat{\nabla}^2\tilde{\omega}_z, \tag{29b}$$

$$(\bar{\gamma}_d + \alpha\,\bar{\Omega}_\theta)\,\tilde{\zeta} - (1 - 2\bar{\Omega}_\theta)\,\tilde{\omega}_z - \frac{\tilde{n}}{2} = \frac{4}{3}\hat{\nabla}^2\tilde{\zeta}, \tag{29c}$$

where

$$\alpha = \frac{\mathrm{i}\,(\Omega - m\Omega_\theta)}{\Omega_\theta}, \tag{30a}$$

$$\bar{\gamma}_d = \frac{\gamma_d}{\Omega_c}, \tag{30b}$$

$$\hat{\nabla}^2 = \frac{\nu}{\Omega_c}\nabla^2. \tag{30c}$$

Suppose, as seems reasonable, that the flow damping rate due to magnetic field asymmetries is much less than the cyclotron frequency; *i.e.*, $|\bar{\gamma}_d| \ll 1$. Suppose, in addition, that the resonance condition $\Omega = m\,\Omega_\theta$ is almost satisfied; *i.e.*, $|\alpha| \ll 1$. In this limit, Eqs. (29) yield

$$\tilde{n} \simeq -2(1 - 2\bar{\Omega}_\theta)\,\tilde{\omega}_z, \tag{31a}$$

$$\tilde{\zeta} \simeq \frac{2\alpha\,\bar{\Omega}_\theta\,(1-2\bar{\Omega}_\theta)}{\bar{n}}\,\tilde{\omega}_z, \tag{31b}$$

$$\hat{\nabla}^2\tilde{\omega}_z \simeq \left(\bar{\gamma}_d + \kappa\,\alpha\,\bar{\Omega}_\theta\right)\tilde{\omega}_z. \tag{31c}$$

Linearization of Eq. (5) gives

$$(1-\bar{\Omega}_\theta)\left(\nabla\tilde{\psi} + \tilde{\boldsymbol{v}}\wedge\hat{\boldsymbol{z}}\right) = \alpha\,\bar{\Omega}_\theta\,\tilde{\boldsymbol{v}} - \hat{\nabla}^2\tilde{\boldsymbol{v}} + \bar{\gamma}_d\,\tilde{\boldsymbol{v}} \sim O(\alpha)\,\tilde{\boldsymbol{v}}, \tag{32}$$

where

$$\tilde{\psi} = -\frac{\tilde{\phi}}{B_z(1-\bar{\Omega}_\theta)}, \tag{33}$$

and $\tilde{\phi}$ is the perturbed electric scalar potential. It follows from Eq. (32) that

$$\tilde{\boldsymbol{v}} = \nabla\tilde{\psi}\wedge\hat{\boldsymbol{z}}\,[1+O(\alpha)\,]\,. \tag{34}$$

Thus, the perturbed flow is divergence free to lowest order in α, and can, therefore, be written in terms of a stream function $\tilde{\psi}$. Note that

$$\tilde{\omega}_z \simeq -\nabla^2\tilde{\psi}\,[1+O(\alpha)\,]\,. \tag{35}$$

It is easily demonstrated from Eq. (26) that

$$t_\theta(r) = \frac{m}{2}\frac{\partial}{\partial r}\left[\mathrm{Im}\left(r\,\frac{\partial\tilde{\psi}}{\partial r}\,\tilde{\psi}^*\right)\right][1+O(\alpha)\,]\,. \tag{36}$$

G The perturbed stream function

Let

$$\tilde{\psi}(r,\theta,t) = \tilde{\psi}(r)\exp[\,\mathrm{i}\,(m\theta-\Omega t)], \tag{37a}$$

$$\tilde{\omega}_z(r,\theta,t) = \tilde{\omega}_z(r)\exp[\,\mathrm{i}\,(m\theta-\Omega t)], \tag{37b}$$

$$\tilde{\phi}(r,\theta,t) = \tilde{\phi}(r)\exp[\,\mathrm{i}\,(m\theta-\Omega t)]. \tag{37c}$$

Equation (31)(c) reduces to

$$\frac{1}{r}\frac{d}{dr}\left(r\,\frac{d\tilde{\omega}_z}{dr}\right) - \frac{m^2}{r^2}\,\tilde{\omega}_z - \frac{\beta}{a^2}\,\tilde{\omega}_z \simeq 0, \tag{38}$$

where

$$\beta = \frac{-\mathrm{i}\,\kappa\,(\Omega - m\,\Omega_\theta) + \gamma_d}{\gamma_\nu}, \tag{39}$$

and

$$\gamma_\nu = \frac{\nu}{a^2}. \tag{40}$$

The most general solution to Eq. (38) which is well behaved in the limit $r \to 0$ takes the form

$$\tilde{\omega}_z(r) \simeq A\,\frac{2|m|}{a^2}\,\frac{I_{|m|}(\sqrt{\beta}\,r/a)}{I_{|m|}(\sqrt{\beta})}, \tag{41}$$

where A is a constant, I_m is a standard Bessel function, and

$$|\mathrm{arg}(\sqrt{\beta})| \leq \frac{\pi}{2}. \tag{42}$$

According to Eq. (35),

$$\frac{1}{r}\frac{d}{dr}\left(r\,\frac{d\tilde{\psi}}{dr}\right) - \frac{m^2}{r^2}\,\tilde{\psi} \simeq -\tilde{\omega}_z. \tag{43}$$

The solution to this equation which is well behaved in the limit $r \to 0$ is

$$\begin{aligned}\tilde{\psi}(r) \quad &\simeq \quad A\left(\frac{r}{a}\right)\left(\frac{I_{|m|+1}(\sqrt{\beta}\,r/a) - I_{|m|-1}(\sqrt{\beta}\,r/a)}{\sqrt{\beta}\,I_{|m|}(\sqrt{\beta})}\right)\\ &\quad + \left(\frac{r}{a}\right)^{|m|}\left(\Psi_m + A\,\frac{I_{|m|-1}(\sqrt{\beta})}{\sqrt{\beta}\,I_{|m|}(\sqrt{\beta})}\right),\end{aligned} \tag{44}$$

where Ψ_m is a constant which parameterizes the strength of the external perturbation.

The physical constraint which must be imposed at the plasma/vacuum interface, located at $r = a$, is that there is zero viscous angular momentum flux normal to the boundary. Thus,

$$\left[r\,\frac{\partial}{\partial r}\left(\frac{\tilde{v}_\theta}{r}\right) + \frac{1}{r}\frac{\partial \tilde{v}_r}{\partial \theta}\right]_a = 0, \tag{45}$$

which reduces to

$$\left(r^2\,\frac{d^2\tilde{\psi}}{dr^2} - r\,\frac{d\tilde{\psi}}{dr} + m^2\,\tilde{\psi}\right)_a \simeq 0. \tag{46}$$

Equations (44) and (46) yield

$$\begin{aligned}\tilde{\psi}(r) \quad &\simeq \quad \Psi_m\,\left(\frac{r}{a}\right)\,Y_m(\beta)\,\left(\frac{I_{|m|+1}(\sqrt{\beta}\,r/a) - I_{|m|-1}(\sqrt{\beta}\,r/a)}{\sqrt{\beta}\,I_{|m|}(\sqrt{\beta})}\right)\\ &\quad +\Psi_m\,\left(\frac{r}{a}\right)^{|m|}\,\left(1 + Y_m(\beta)\,\frac{I_{|m|-1}(\sqrt{\beta})}{\sqrt{\beta}I_{|m|}(\sqrt{\beta})}\right),\end{aligned} \tag{47}$$

where

$$Y_m(\beta) = \frac{A}{\Psi_m} = \frac{(|m|-1)}{1-(|m|+1)\,Z_m(\beta)}, \tag{48}$$

and

$$Z_m(\beta) = \frac{I_{|m|+1}(\sqrt{\beta})}{\sqrt{\beta}\,I_{|m|}(\sqrt{\beta})}. \tag{49}$$

H Intrinsic stability

Suppose that there is no external perturbation; *i.e.*, $\Psi_m = 0$. Let

$$\Omega = m\,\Omega_\theta + \mathrm{i}\,\gamma, \tag{50}$$

where γ is the growth rate. It follows that

$$\beta = \frac{\kappa\,\gamma + \gamma_d}{\gamma_\nu}. \tag{51}$$

For $\beta > 0$, the most general solution to the perturbed vorticity equation, (38), is

$$\tilde{\omega}_z(r) \simeq A\,\frac{2|m|}{a^2}\,\frac{I_{|m|}(\sqrt{\beta}\,r/a)}{I_{|m|}(\sqrt{\beta})}. \tag{52}$$

The instability criterion (which leaves A finite whilst $\Psi_m \to 0$ in Eq. (48)) is

$$(|m|+1)\,Z_m(\beta) = \frac{(|m|+1)}{\sqrt{\beta}}\,\frac{I_{|m|+1}(\sqrt{\beta})}{I_{|m|}(\sqrt{\beta})} \simeq 1. \tag{53}$$

This criterion is never satisfied for any integer m and real positive β, implying that a rigidly rotating plasma is intrinsically stable. Thus, it is reasonable to assume that the only mode present in the plasma is that imposed externally.

For $\beta < 0$, the most general solution of the perturbed vorticity equation is

$$\tilde{\omega}_z(r) \simeq A\,\frac{2|m|}{a^2}\,\frac{J_{|m|}(\sqrt{-\beta}\,r/a)}{J_{|m|}(\sqrt{-\beta})}, \tag{54}$$

where J_m is a standard Bessel function. By a straightforward generalization of the previous result, the dispersion relation for stable modes takes the form

$$\frac{(|m|+1)}{\sqrt{-\beta}}\,\frac{J_{|m|+1}(\sqrt{-\beta})}{J_{|m|}(\sqrt{-\beta})} \simeq 1. \tag{55}$$

There are many roots of this dispersion relation with real negative values of β. These roots correspond to modes with the negative growth rates

$$\gamma = \frac{\beta\,\gamma_\nu - \gamma_d}{\kappa}. \tag{56}$$

Table I shows the first few roots of (*i.e.*, values of $\sqrt{-\beta}$ which satisfy) Eq. (55) calculated for $m = 1, 2$, and 3. It is clear from the above analysis that the steady state cross section of a plasma confined in a Penning-Malmberg trap is necessarily circular. Any ellipticity ($m = 2$), triangularity ($m = 3$), *etc.* decays away under the action of viscosity. It is also clear that the circular stream surfaces of the plasma must be concentric, since any lack of concentricity ($m = 1$) is also eliminated by viscosity.

I Axisymmetric perturbations

Consider axisymmetric (*i.e.*, $m = 0$) perturbations about a rigid rotator state. The analysis of Section II.F remains valid for $m = 0$. Hence, the perturbed vorticity satisfies (see Eq. (38))

$$\frac{1}{r}\frac{d}{dr}\left(r\,\frac{d\tilde{\omega}_z}{dr}\right) - \frac{\beta}{a^2}\,\tilde{\omega}_z \simeq 0. \tag{57}$$

The solution of this equation is

$$\tilde{\omega}_z \simeq A\,I_0\left(\sqrt{\beta}\,\frac{r}{a}\right) \tag{58}$$

for $\beta > 0$, and

$$\tilde{\omega}_z \simeq A\,J_0\left(\sqrt{-\beta}\,\frac{r}{a}\right) \tag{59}$$

for $\beta < 0$. Here, A is a constant. Now,

$$\tilde{\omega}_z \simeq \frac{1}{r}\frac{d(r^2\,\tilde{\Omega}_\theta)}{dr}, \tag{60}$$

where $\tilde{\Omega}_\theta(r)$ is the perturbed angular velocity of the plasma. It is easily demonstrated that

$$\tilde{\Omega}_\theta(r) \simeq A\,\frac{I_1(\sqrt{\beta}\,r/a)}{\sqrt{\beta}\,r/a} \tag{61}$$

for $\beta > 0$, and

$$\tilde{\Omega}_\theta(r) \simeq A\,\frac{J_1(\sqrt{-\beta}\,r/a)}{\sqrt{-\beta}\,r/a} \tag{62}$$

for $\beta < 0$. The physical constraint imposed at the plasma/vacuum interface is (see Eq. (45))

$$\frac{d\tilde{\Omega}_\theta(a)}{dr} = 0. \tag{63}$$

This constraint yields the dispersion relation

$$\frac{2}{\sqrt{\beta}}\,\frac{I_1(\sqrt{\beta})}{I_0(\sqrt{\beta})} \simeq 1 \tag{64}$$

for $\beta > 0$, and

$$\frac{2}{\sqrt{-\beta}}\,\frac{J_1(\sqrt{-\beta})}{J_0(\sqrt{-\beta})} \simeq 1 \tag{65}$$

for $\beta < 0$.

The dispersion relation (64) is never satisfied for any real positive values of β. There are many roots of the dispersion relation (65) with real negative values of β. These roots correspond to modes with the negative growth rates

$$\gamma = \frac{\beta\,\gamma_\nu - \gamma_d}{\kappa}. \tag{66}$$

Table II shows the first few roots of Eq. (65). It is clear from the above analysis that any small deviation of the plasma angular velocity profile from that of a rigid rotator decays away under the action of viscosity.

J The perturbed electric field

In the vacuum region outside the plasma

$$\frac{1}{r}\frac{d}{dr}\left(r\,\frac{d\tilde{\phi}}{dr}\right) - \frac{m^2}{r^2}\,\tilde{\phi} = 0, \tag{67}$$

which implies that

$$\tilde{\phi}(r > a) = \Phi_m\left(\frac{r}{a}\right)^{|m|} + \Phi_{-m}\left(\frac{r}{a}\right)^{-|m|}, \tag{68}$$

where $\Phi_{\pm m}$ are constants. Matching the perturbed electric potential in the vacuum region to that inside the plasma yields

$$\tilde{\phi}(a) \simeq -B_z\,(1-\bar{\Omega}_\theta)\,\tilde{\psi}(a), \tag{69a}$$

$$\frac{d\tilde{\phi}(a)}{dr} \simeq -B_z\,(1-\bar{\Omega}_\theta)\,\frac{d\tilde{\psi}(a)}{dr}, \tag{69b}$$

where use has been made of Eq. (33). According to the analysis of Section II.G,

$$\tilde{\psi}(a) \simeq \Psi_m\,(1+Y_m(\beta)Z_m(\beta)\,)\,, \tag{70a}$$

$$\frac{r}{|m|}\frac{d\tilde{\psi}}{dr}\bigg|_a \simeq \Psi_m\,(1-Y_m(\beta)Z_m(\beta)\,)\,. \tag{70b}$$

Thus,

$$\Phi_m \simeq -B_z\,(1-\bar{\Omega}_\theta)\,\Psi_m, \tag{71a}$$

$$\Phi_{-m} \simeq -B_z\,(1-\bar{\Omega}_\theta)\,Y_m(\beta)\,Z_m(\beta)\,\Psi_m, \tag{71b}$$

and

$$\tilde{\phi}(r>a) \simeq \Phi_m\left[\left(\frac{r}{a}\right)^{|m|}+Y_m(\beta)Z_m(\beta)\left(\frac{r}{a}\right)^{-|m|}\right], \tag{72}$$

where Φ_m parameterizes the strength of the externally imposed electric field.

Suppose that the external electric field is generated by a set of electrodes of negligible radial extent located at radius $r_c > a$. For the sake of simplicity, the electrodes are assumed to be connected to feedback controlled circuits which maintain in them a radially integrated charge density $\sigma(\theta)\exp(-\mathrm{i}\,\Omega\,t)$. In this situation, Eq. (72) only holds in the region $a < r \leq r_c$. In the region outside the electrodes

$$\tilde{\phi}(r>r_c) \simeq \Phi_m\left[\left(\frac{r_c}{a}\right)^{|m|}\left(\frac{r}{r_c}\right)^{-|m|}+Y_m(\beta)Z_m(\beta)\left(\frac{r}{a}\right)^{-|m|}\right]. \tag{73}$$

It is readily demonstrated from Poisson's equation that

$$\Phi_m = \frac{r_c}{2|m|\,\epsilon_0}\left(\frac{a}{r_c}\right)^{|m|}\oint\sigma(\theta)\,\exp(-\mathrm{i}\,m\theta)\,\frac{d\theta}{2\pi}. \tag{74}$$

K The angular equation of motion

The angular equation of motion of the plasma follows from Eqs. (15), (25), (36), (70), (71):

$$\kappa\,\frac{\partial\Omega_\theta}{\partial t} \simeq \sum_m \frac{4m^2\,|\Phi_m|^2}{B_z{}^2(1-\bar{\Omega}_\theta)^2a^4}\,T_m(\beta)-\gamma_d\,\Omega_\theta, \tag{75}$$

where

$$\bar{n}\, a^2 = \text{constant}, \tag{76}$$

and

$$\begin{aligned} T_m(\beta) &= -\text{sgn}(m)\, \text{Im}\,(\, Z_m(\beta)\, Y_m(\beta)\,) \\ &= -\text{sgn}(m)\,(|m|-1)\, \text{Im}\left(\frac{Z_m(\beta)}{1-(|m|+1)\, Z_m(\beta)}\right). \end{aligned} \tag{77}$$

Note that neither an $m = 0$ nor an $|m| = 1$ perturbation are able to exert a torque on the plasma. In the former case the perturbation is axisymmetric, so there is no $\tilde{E}_\theta$ to accelerate the plasma in the θ direction. In the latter case the perturbation merely imparts a rigid shift to the plasma, without distortion of the stream surfaces.

L The torque function

According to Eq. (75), the torque exerted on the plasma by the mth harmonic of the external electric field is proportional to the function $T_m(\beta)$, which is specified in Eq. (77). Now, the asymptotic behaviour of the function $Z_m(\beta)$ is

$$Z_m(\beta) \to \frac{1}{2(|m|+1)}\left(1 - \frac{\beta}{4(|m|+1)(|m|+2)} + \cdots\right), \tag{78}$$

for $|\beta| \ll 1$, and

$$Z_m(\beta) \to \frac{1}{\sqrt{\beta}} \tag{79}$$

for $|\beta| \gg 1$. It follows from Eqs. (39), (78), and (79) that

$$T_m(\beta) \to \frac{|m|(|m|-1)}{2(|m|+1)^2(|m|+2)}\,\frac{\kappa\,(\Omega_\theta - \Omega/m)}{\gamma_\nu} \tag{80}$$

for $|\beta| \ll 1$, and

$$\begin{aligned} T_m(\beta) \;\to\; & -\text{sgn}(m)\,(|m|-1)\, \sin\left[(1/2)\, \tan^{-1}(\,\kappa\,[\Omega - m\,\Omega_\theta]/\gamma_d)\,\right] \\ & \times \left(\frac{{\gamma_\nu}^2}{\kappa^2(\Omega - m\,\Omega_\theta)^2 + {\gamma_d}^2}\right)^{1/4} \end{aligned} \tag{81}$$

for $|\beta| \gg 1$.

In most Penning-Malmberg traps the time scale on which the plasma spins down due to asymmetries in the magnetic field is much longer than the time scale required for viscous relaxation of the velocity profile; *i.e.*, $\gamma_d \ll \gamma_\nu$.[9] In this limit,

$$T_m \simeq \frac{|m|(|m|-1)}{2(|m|+1)^2(|m|+2)}\,\frac{\kappa\,(\Omega_\theta - \Omega/m)}{\gamma_\nu}, \tag{82}$$

for $|\Omega_\theta - \Omega/m| \ll \gamma_\nu$ (assuming that $\kappa \sim O(1)$), and

$$T_m \simeq \mathrm{sgn}(\Omega_\theta - \Omega/m)\,\frac{(|m|-1)}{\sqrt{2}}\sqrt{\frac{\gamma_\nu}{|m|\,\kappa\,|\Omega_\theta - \Omega/m|}} \tag{83}$$

for $|\Omega_\theta - \Omega/m| \gg \gamma_\nu$. The variation of the torque function T_m with the plasma angular velocity Ω_θ is sketched in Figure 1. The mth harmonic of the externally imposed electric field resonates with the plasma when its angular phase velocity Ω/m matches the angular velocity Ω_θ of the plasma. At resonance, zero torque is exerted on the plasma. As the velocity difference between the plasma and the electric field is gradually increased, the torque initially increases linearly with the velocity difference, reaches a maximum value, and then decreases like one over the square root of the velocity difference. The width of the peak (in units of angular velocity) is of order γ_ν; *i.e.*, the width is determined by the plasma viscosity. In conventional Penning-Malmberg trap experiments the typical time scale for viscous relaxation of the plasma velocity profile is much longer than the rotation period; *i.e.*, $\gamma_\nu \ll |\Omega_\theta|$.[9] This implies that the mth harmonic of the externally imposed electric field is only able to exert a significant torque on the plasma when it is very close to resonance; *i.e.*, when its angular phase velocity almost matches the angular rotation velocity of the plasma. Thus, the "close to resonance" ordering $|\alpha| \ll 1$, adopted in Section II.F, is reasonable, since if $|\alpha| \sim O(1)$ then the relevant harmonic of the external field is so far from resonance that it exerts virtually no torque on the plasma.

The most surprising aspect of Fig. 1 is the *direction* of the torque. The torque is *negative* when the external electric field rotates *faster* than the plasma (*i.e.*, $\Omega/m > \Omega_\theta$), and *positive* when the external field rotates *slower* than the plasma (*i.e.*, $\Omega/m < \Omega_\theta$). At first sight, this result appears somewhat counter-intuitive. One might expect a field which rotates faster than the plasma to exert

a positive torque so as to bring the plasma into resonance, and *vice versa*. (This is certainly what occurs in a conventional electron-ion plasma subjected to an externally imposed, rotating, non-axisymmetric, magnetic field.[19]) However, it is demonstrated in Section II.O that this direction of the torque is entirely consistent with a standard result in hydrodynamic theory.

The torque function T_m attains its maximum amplitude, $T_m(\max)$, when $|\Omega_\theta - \Omega/m| = g_m\,\gamma_\nu/\kappa$. Table III shows the quantities g_m and $T_m(\max)$, calculated for various values of m. It can be seen that both g_m and $T_m(\max)$ increase gradually with increasing poloidal mode number.

The limit $\gamma_d \gg \gamma_\nu$ is not particularly relevant to Penning-Malmberg trap experiments, but is worth examining for the sake of completeness. In this limit,

$$T_m \simeq \frac{|m|(|m|-1)}{2}\,\frac{\kappa\,(\Omega_\theta - \Omega/m)}{\gamma_d}\sqrt{\frac{\gamma_\nu}{\gamma_d}} \tag{84}$$

for $|\Omega_\theta - \Omega/m| \ll \gamma_d$, and

$$T_m \simeq \mathrm{sgn}(\Omega_\theta - \Omega/m)\,\frac{(|m|-1)}{\sqrt{2}}\sqrt{\frac{\gamma_\nu}{|m|\,\kappa\,|\Omega_\theta - \Omega/m|}} \tag{85}$$

for $|\Omega_\theta - \Omega/m| \gg \gamma_d$. The variation of the torque function with the plasma angular velocity is similar to that sketched in Fig. 1, except that the width of the resonance (in units of angular velocity) is of order γ_d; *i.e.*, the width is determined by the flow damping rate. The torque function attains its maximum value,

$$T_m(\max) = \frac{(|m|-1)}{\sqrt{8}}\sqrt{\frac{\gamma_\nu}{\gamma_d}}, \tag{86}$$

when

$$|\Omega_\theta - \Omega/m| = \frac{\sqrt{3}\,|m|\,\gamma_d}{\kappa}. \tag{87}$$

Clearly, the drag term γ_d has the effect of widening the peaks of the torque *vs.* angular velocity curve but reducing their amplitude.

M Torque balance

Steady state solutions of the angular equation of motion, (75), satisfy

$$T_{\rm drag}(\Omega_\theta) = T_{\rm EM}(\Omega_\theta), \tag{88}$$

where

$$T_{\rm drag}(\Omega_\theta) = \gamma_d\,\Omega_\theta \tag{89}$$

is proportional to (minus) the drag torque due to asymmetries in the magnetic field, and

$$T_{\rm EM}(\Omega_\theta) = \sum_m \frac{4m^2\,|\Phi_m|^2}{B_z{}^2(1-\bar{\Omega}_\theta)^2 a^4}\,T_m(\beta) \tag{90}$$

is proportional to the electromagnetic torque exerted on the plasma by the externally applied electric field.

As is illustrated in Fig. 2, the steady state angular velocity of the plasma corresponds to one of the crossing points of the drag torque curve, $T_{\rm drag}(\Omega_\theta)$, and the electromagnetic torque curve, $T_{\rm EM}(\Omega_\theta)$. There are either zero or two crossing points associated with each poloidal harmonic of the externally applied electric field, with the exception of the $m = 0$ and $|m| = 1$ harmonics, which exert no torque on the plasma. For each $|m| > 1$ harmonic which possesses two crossing points, the crossing point which lies closest to the resonance, $\Omega_\theta = \Omega/m$, is dynamically unstable, whereas the other crossing point is dynamically stable. Note that all stable crossing points correspond to a situation in which the angular phase velocity of the relevant poloidal harmonic of the external electric field is slightly less than the plasma angular velocity.

Consider the physically relevant limit $\gamma_\nu/|\Omega_\theta| \rightarrow 0$, in which the various peaks of the electromagnetic torque *vs.* angular velocity curve corresponding to different poloidal harmonics of the external electric field are well separated. For each harmonic of the externally applied electric field there is a *minimum* amplitude of the poloidal electric field at the plasma edge,

$$|\tilde{E}_{\theta\,m}| = \frac{|m|\,|\Phi_m|}{a}, \tag{91}$$

required to balance the drag torque with $\Omega_\theta \simeq \Omega/m$. This critical amplitude is given by

$$|\tilde{E}_{\theta\, m}|_{\rm min} \simeq \frac{B_z\,|1-\bar{\Omega}_\theta|}{2}\sqrt{\frac{\gamma_d\,|\Omega|\,a^2}{|m|\,T_m({\rm max})}}, \tag{92}$$

where $T_m(\max)$ is tabulated in Table III. If $|\tilde{E}_{\theta\, m}|$ falls below its critical value then the steady state solution is lost, and the plasma starts to spin down. The plasma subsequently either comes into equilibrium with a higher $|m|$ harmonic of the external field or spins down indefinitely, leading to an eventual loss of confinement. Note that the critical amplitude is independent of the plasma viscosity.

N Torque profiles

The density per unit length of the non-linear torque exerted by the mth harmonic of the externally applied electric field is given by

$$\hat{t}_\theta(r) \simeq \frac{m}{4\pi r}\frac{\partial}{\partial r}\left[{\rm Im}\left(r\,\frac{\partial\tilde{\psi}}{\partial r}\,\tilde{\psi}^*\right)\right]. \tag{93}$$

Thus, the total torque per unit length acting on the plasma is

$$T_\theta = \int_0^a 2\pi r\,\hat{t}_\theta(r)\,dr. \tag{94}$$

The torque function, T_m, which is discussed in Section II.L, is related to the total torque per unit length via

$$T_\theta = \frac{m^2\,|\Phi_m|^2}{{B_z}^2(1-{\bar{\Omega}_\theta}^2)}\,T_m. \tag{95}$$

Now,

$$T_m = \int_0^1 t_m(r/a)\,d(r/a), \tag{96}$$

where

$$t_m(r/a) = \frac{2\pi r\,t_\theta(r)}{[m^2|\Phi_m|^2/{B_z}^2(1-{\bar{\Omega}_\theta}^2)a]}. \tag{97}$$

Here, $t_m(r/a)\,d(r/a)$ is proportional to the net torque per unit length exerted on the plasma between radii r and $r+dr$. The analysis of Section II.G readily yields

$$\begin{aligned} t_m(x) &= \mathrm{sgn}(m)\,\mathrm{Im}\left[Y_m^*(\beta)\,\frac{I_{|m|}^*(\sqrt{\beta}\,x)}{I_{|m|}^*(\sqrt{\beta})}\right. \\ &\quad\times\left\{Y_m(\beta)\,x^2\,\frac{I_{|m|+1}(\sqrt{\beta}\,x)-I_{|m|-1}(\sqrt{\beta}\,x)}{\sqrt{\beta}\,I_{|m|}(\sqrt{\beta})}\right. \\ &\quad\left.\left.+\,x^{1+|m|}\left(1+Y_m(\beta)\,\frac{I_{|m|-1}(\sqrt{\beta})}{\sqrt{\beta}\,I_{|m|}(\sqrt{\beta})}\right)\right\}\right]. \end{aligned} \tag{98}$$

Figure 3 shows the torque profile $t_m(r/a)$ calculated for $m=2$, $\gamma_d \ll \gamma_\nu$, and various values of

$$\zeta = \frac{\kappa\,(\Omega_\theta - \Omega/m)}{g_m\,\gamma_\nu}, \tag{99}$$

where g_m is specified in Table III. Recall that $|\zeta| = 1$ corresponds to the two plasma angular velocities which give the maximum and minimum torques in Fig. 1. For $|\zeta| \ll 1$, the torque increases linearly with the angular velocity difference between the plasma and the external electric field; *i.e.*, with $\Omega_\theta - \Omega/m$. For $|\zeta| \gg 1$, the torque decreases like one over the square root of the velocity difference. It is clear from Fig. 3 that in the former asymptotic limit the torque exerted on the plasma by the external field is fairly evenly distributed throughout the plasma, whereas in the latter limit the torque is confined to a narrow layer close to the plasma boundary. According to Fig. 2, stable balance points between the electromagnetic torque and the drag torque are only possible when the electromagnetic torque decreases as the magnitude of the angular velocity difference between the plasma and the external field increases. This implies that a steady state solution can only be obtained when the torque exerted on the plasma by the externally applied electric field is mostly concentrated close to the edge of the plasma.

O The effect of angular velocity shear

Suppose that the plasma initially possesses a small amount of angular velocity shear. According to Section II.I, the shear gradually decays away under the action of viscosity. The time asymptotic angular velocity profile of the plasma consists of rigid rotation plus a small admixture of the most slowly decaying eigenfunction of Section II.I. Thus,

$$\Omega_\theta(r,t) = \Omega_{\theta 0}(t)\left(1+\epsilon(t)\,\frac{J_1(\beta_1\,r/a)}{\beta_1\,r/a}\right), \tag{100}$$

where $\beta_1 = 5.136$ (see Table II),

$$\Omega_{\theta\,0}(t) = \Omega_{\theta\,00}\,\mathrm{e}^{-\gamma_d\,t/\kappa}, \tag{101a}$$

$$\epsilon(t) = \epsilon_0\,e^{-{\beta_1}^2\gamma_\nu\,t/\kappa}, \tag{101b}$$

and it is assumed that $\gamma_\nu/|\Omega_{\theta 0}| \ll |\epsilon| \ll 1$.

Linear analysis, along the lines of Section II.F, in which $O(\epsilon)$ is neglected with respect to $O(1)$ (ϵ replaces α as the ordering parameter in the analysis) yields

$$[\Omega_\theta(r,t) - \Omega/m]\,\nabla^2\tilde{\psi} - G(r,t)\,\tilde{\psi} \simeq -\mathrm{i}\,\frac{\nu}{m\kappa}\nabla^4\,\tilde{\psi} + \mathrm{i}\,\frac{\gamma_d}{m\kappa}\,\nabla^2\tilde{\psi}, \tag{102}$$

where

$$G(r,t) = \frac{1}{r^3}\frac{\partial}{\partial r}\left(r^3\,\frac{\partial\,\Omega_\theta(r,t)}{\partial r}\right) = -\Omega_{\theta 0}\,\epsilon\,\frac{{\beta_1}^2}{a^2}\,\frac{J_1(\beta_1\,r/a)}{\beta_1\,r/a}. \tag{103}$$

Equation (102) is the equivalent to Eq. (38) in the presence of velocity shear.

The ratio of the terms on the right hand side of Eq. (102) to those on the left hand side is $O(\gamma_\nu/\epsilon|\Omega_{\theta 0}|)$ which, by assumption, is a very small number. Thus, to a good approximation the dissipative terms can be neglected in Eq. (102), which then reduces to the well known *diocotron equation*[20]

$$\frac{d^2\tilde{\psi}}{dr^2} + \frac{1}{r}\frac{d\tilde{\psi}}{dr} - \frac{m^2}{r^2}\,\tilde{\psi} - \frac{G(r,t)}{\Omega_\theta(r,t) - \Omega/m}\,\tilde{\psi} = 0. \tag{104}$$

This equation is clearly singular on the *critical surface*, $r = r_s$, where

$$\Omega_\theta(r_s,t) = \Omega/m. \tag{105}$$

The singularity is resolved in a thin *critical layer*, centred on the critical surface, in which dissipative effects are important. The physical solution is obtained via asymptotic matching between the solution of the diocotron equation and the critical layer solution.

Let

$$x = (r - r_s)/r_s. \tag{106}$$

At any given time, the most general solution of the diocotron equation in the vicinity of the critical surface is written

$$\begin{aligned}\tilde{\psi}(x) \quad &\simeq \quad \Psi_s \left(1 + \lambda_s\, x\, (\ln|x| - 1) + O(x^2)\right) \\ &\qquad + \Psi_s' \left(x + (\lambda_s - 1)\, x^2/2 + O(x^3)\right),\end{aligned} \tag{107}$$

where

$$\lambda_s = \left(\frac{r\, G}{\Omega_\theta'}\right)_{r_s} \tag{108}$$

and $\Omega_\theta' \equiv \partial\Omega_\theta/\partial r$. Here, Ψ_s is termed *the coefficient of the large solution* and Ψ_s' is termed *the coefficient of the small solution.* In principle, these coefficients can be different on either side of the critical surface. The jump in the coefficients is fixed by asymptotic matching to the critical layer solution. However, in the small ϵ limit, for which the perturbed flow is divergence free to lowest order, critical layer solutions permit a jump in the coefficient of the small solution but forbid a similar jump in the coefficient of the large solution. It is convenient to parameterize the jump in the coefficient of the small solution via

$$\Delta_s = \frac{\Psi_{s+}' - \Psi_{s-}'}{\Psi_s}, \tag{109}$$

where Ψ_{s+}' denotes the coefficient of the small solution to the right (*i.e.*, $r > r_s$) of the critical surface, *etc.* It is demonstrated in Appendix A that the critical layer solution requires Δ_s to take the value

$$\Delta_s = \mathrm{i}\, \pi \sigma_s \lambda_s, \tag{110}$$

where $\sigma_s = \mathrm{sgn}(m)\, \mathrm{sgn}(\Omega_\theta'(r_s))$. Note that this expression is *independent* of viscosity, despite the fact that viscosity determines the width, δ_s, of the critical

layer. In fact,

$$\frac{\delta_s}{a} \sim \left(\frac{\gamma_\nu}{|m|\,\kappa\,a\,|\Omega_\theta'(r_s)|}\right)^{1/3}. \tag{111}$$

The torque density acting inside the plasma is measured by (see Eq. (36))

$$t_\theta(r) \simeq \frac{m}{2}\frac{\partial}{\partial r}\left[\mathrm{Im}\left(r\,\frac{\partial\tilde{\psi}}{\partial r}\,\tilde{\psi}^*\right)\right]. \tag{112}$$

It is easily demonstrated that this expression is zero in any region of the plasma in which the perturbation is governed by the diocotron equation. Thus, no torque is exerted in the plasma except in the immediate vicinity of the critical surface where the diocotron equation breaks down. The integrated torque exerted across the critical layer is measured by

$$T_s = \frac{4}{a^4}\int_{r_{s-}}^{r_{s+}} t_\theta(r)\,dr = \frac{2m}{a^4}\,\mathrm{Im}(\Delta_s)\,|\Psi_s|^2. \tag{113}$$

It follows from Eq. (110) that

$$T_s = \frac{2\pi\,|m|\,|\Psi_s|^2}{a^4}\,\frac{r_s\,G(r_s,t)}{|\Omega_\theta'(r_s,t)|}. \tag{114}$$

An analogous result to this was first derived by in hydrodynamic theory by Tollmein in the 1920's.[21] See also Foote & Lin.[22]

It is clear from Eq. (114) that the sign of the torque exerted in the vicinity of a critical layer is determined by the local sign of the function $G(r,t)$. The physical significance of this function is most readily appreciated by writing down the angular equation of motion of the plasma, which takes the form

$$\kappa\,\frac{\partial\,\Omega_\theta(r)}{\partial t} \simeq \frac{T_s\,a^4}{4\,{r_s}^3}\,\delta(r-r_s) + \nu\,G(r,t) - \gamma_d\,\Omega_\theta(r). \tag{115}$$

Here, the small but finite thickness of the critical layer has been neglected for the sake of simplicity. A comparison of Eqs. (114) and (115) shows that *the torque exerted at the critical surface always acts in the same direction as the local viscous*

torque. There is an underlying physical reason for this result. Imagine that the plasma is strongly perturbed from equilibrium so that it acquires a large amount of angular velocity shear. Viscosity acts to reduce this shear and eventually returns the plasma to a rigid rotator state. However, for strong perturbations the plasma becomes unstable to modes driven by the velocity shear. (Note that for the small levels of velocity shear considered in this paper the plasma remains stable, as evinced by the lack of modes with positive growth rates in Section II.I.) These modes are able to rapidly redistribute angular momentum by means of momentum injection into the various critical layers which develop inside the plasma. (Note that the behaviour of critical layers is essentially independent of whether the perturbation is externally imposed or due to some naturally occurring instability.) The fact that the torque exerted at a critical layer is always in the same direction as the local viscous torque ensures that the unstable modes always act to relax the plasma angular velocity profile back to that of a rigid rotator, thereby, eventually stabilizing themselves. Thus, the sign of the torque in Eq. (114) is entirely consistent with d'Alembert's principle.

Consider the case $\epsilon > 0$, where the inside of the plasma spins slightly faster than the outside. It is clear from Eq. (103) and (114) that the torque exerted on the plasma is only *positive* when the critical surface lies towards the outside of the plasma (*i.e.*, when $r_s > 0.746\,a$), and most of the plasma is, therefore, spinning *faster* than the external perturbation. Likewise, the torque is *negative* when $r_s < 0.746\,a$, and most of the plasma is, therefore, spinning *slower* than the external perturbation. Similar behaviour is obtained for the $\epsilon < 0$ case. This behaviour is entirely consistent with that already found for the zero shear case, where the torque is positive when *all* of the plasma is spinning faster than the external perturbation, and *vice versa*.

Note that zero torque is exerted on the plasma when the radius of the critical surface lies at $0.746\,a$ (*i.e.*, the radius at which $J_1(\beta_1\,r/a) = 0$). However, this equilibrium point is dynamically unstable. Consider the $\epsilon > 0$ case. If the perturbation slows down slightly then the radius of the critical surface moves outward and angular momentum is injected into the plasma, tending to spin it up. Likewise, if the perturbation speeds up slightly then the radius of the critical surface decreases and angular momentum is extracted from the plasma, tending to slow it down.

If there is no critical surface inside the plasma then the final term on the left hand side of Eq. (104) is $O(\epsilon)$ smaller than the other terms, and can, therefore, be neglected. To lowest order, the solution of this equation which satisfies the boundary conditions (69) is given by

$$\tilde{\psi}(r) \simeq -\frac{\Phi_m}{B_z\,(1-\bar{\Omega}_\theta)}\left(\frac{r}{a}\right)^{|m|}, \tag{116}$$

and zero torque is exerted on the plasma. However, this solution is not quite correct since it does not satisfy the boundary condition (46) at the plasma/vacuum interface. In order to achieve this a thin boundary layer develops at the edge of the plasma. The external perturbation is then able to exert a relatively small torque on this layer. It is easily demonstrated that the correct solution is

$$\tilde{\psi}(r) \simeq -\frac{\Phi_m}{B_z\,(1-\bar{\Omega}_\theta)}\left[\left(\frac{r}{a}\right)^{|m|}\left(1+\frac{|m|-1}{ka}\right)-\frac{2|m|(|m|-1)}{(ka)^2}\,e^{k\,(r-a)}\right] \tag{117}$$

for $r \leq a$, and

$$\tilde{\psi}(r) \simeq -\frac{\Phi_m}{B_z\,(1-\bar{\Omega}_\theta)}\left[\left(\frac{r}{a}\right)^{|m|}+\frac{|m|-1}{ka}\left(\frac{r}{a}\right)^{-|m|}\right] \tag{118}$$

for $r > a$. Here,

$$k = \frac{e^{\mathrm{i}\,\sigma_a\,\pi/4}}{\delta_a}, \tag{119}$$

where $\sigma_a = \mathrm{sgn}(\Omega_\theta(a) - \Omega/m)\,\mathrm{sgn}(m)$, and

$$\delta_a = a\sqrt{\frac{\gamma_\nu}{|m|\,\kappa\,|\Omega_\theta(a)-\Omega/m|}} \tag{120}$$

is the layer width. The above solution is only valid when $\delta_a/a \ll 1$.

The integrated torque exerted in the edge boundary layer is measured by

$$T_a = \frac{4}{a^4}\int_{a-}^{a+} t_\theta(r)\,dr. \tag{121}$$

It is easily demonstrated that

$$T_a \simeq \mathrm{sgn}(\Omega_\theta(a) - \Omega/m)\,\frac{4m^2|\Phi_m|^2}{B_z{}^2(1-\bar{\Omega}_\theta)^2 a^4}\,\frac{|m|-1}{\sqrt{2}}\,\frac{\delta_a}{a}. \tag{122}$$

Note that this expression is identical to the $|\Omega_\theta - \Omega/m| \gg \gamma_\nu$ limit in the case of zero velocity shear, except that here the angular rotation velocity of the plasma is represented by its edge value (*i.e.*, $\Omega_\theta \to \Omega_\theta(a)$).

It is helpful to parameterize the total torque per unit length exerted on the plasma using $\hat{T}$, where

$$T = \frac{4}{a^4}\int_0^a t_\theta(r)\,dr = \frac{4\,m^2\,|\Phi_m|^2}{B_z{}^2\,(1-\bar{\Omega}_\theta)^2\,a^4}\,\hat{T}. \tag{123}$$

It is possible to identify two limits. In the first limit the angular phase velocity of the external perturbation is such that a critical layer forms well inside the plasma. In this case, the width of the critical layer is of order

$$\frac{\delta_s}{a} \sim \left(\frac{\gamma_\nu}{\epsilon\,\Omega_{\theta 0}}\right)^{1/3}, \tag{124}$$

and $\hat{T} \sim O(1)$ (assuming that $\Psi_s \sim \psi(a)$). In the second limit the angular phase velocity of the external perturbation is such that no region of the plasma is close to resonance. In this case, an edge boundary layer whose thickness is of order

$$\frac{\delta_a}{a} \sim \left(\frac{\gamma_\nu}{\Omega_{\theta 0}}\right)^{1/2} \tag{125}$$

forms, and

$$\hat{T} \sim \left(\frac{\gamma_\nu}{\Omega_{\theta 0}}\right)^{1/2} \ll 1. \tag{126}$$

As the critical layer moves towards the edge of the plasma it widens because the plasma angular velocity shear tends to zero as $r \to a$. A similar phenomenon occurs as the critical layer moves towards the axis of rotation of the plasma. The layer overlaps the edge (axis) when

$$\frac{\delta_s}{a} \sim \frac{a-r_s}{a} \sim \frac{r_s}{a} \sim \left(\frac{\gamma_\nu}{\epsilon\,\Omega_{\theta 0}}\right)^{1/4}. \tag{127}$$

At this point the critical layer is approximately as wide as the edge boundary layer, and

$$\hat{T} \sim \left(\frac{\gamma_\nu}{\epsilon\,\Omega_{\theta 0}}\right)^{1/4}, \tag{128}$$

with approximately equal contributions coming from the critical layer and the edge boundary layer.

P Numerical results

A shooting code has been developed which solves Eq. (102), subject to the boundary condition (46), and evaluates the torque acting on the plasma directly, using Eq. (36). The input parameters to the code are the poloidal mode number m, the normalized shear

$$\alpha_1 = \frac{m\,\kappa\,\Omega_{\theta 0}\,\epsilon}{\gamma_\nu}, \tag{129}$$

and the angular velocity parameter

$$z = \frac{m\,\kappa}{\gamma_\nu}\left(\Omega_{\theta 0} - \frac{\Omega}{m}\right). \tag{130}$$

The width of a critical layer is of order $\alpha_1^{-1/3}\,a$, whereas the width of an edge layer is of order $\alpha_1^{-1/4}\,a$. Numerical difficulties arise if either type of layer becomes extremely thin compared to the plasma radius. These difficulties can only be avoided if the shear parameter α_1 is limited to lie in the range $|\alpha_1| \lesssim 10^4$. The output from the code *exactly* matches the analytic result (77) for the case of zero velocity shear ($\alpha_1 = 0$). Furthermore, for the case of (relatively) strong velocity shear ($\alpha_1 \gg 1$) the output from the code is in complete agreement with the preceding analysis. For instance, Fig. 4 shows the normalized torque density ($\hat{t}(r/a)$, where $\hat{T} = \int_0^1 \hat{t}(r/a)\,d(r/a)$, and the normalized torque $\hat{T}$ is defined in Eq. (123)) plotted as a function of the major radius for $m = 2$, $\alpha_1 = 10^4$, and $z = -500$. It can be seen that, as predicted above, the torque is exerted in a relatively narrow layer centred on the critical surface ($r_s = 0.666\,a$). Figure 5 shows the normalized torque exerted on the plasma $\hat{T}$ plotted as a function of the radius of the critical surface r_s for $m = 2$ and $\alpha_1 = 2000$. Recall that analytic

theory predicts that in the $\alpha_1 \gg 1$ limit the torque exerted on the plasma should be negative when the critical surface lies towards the centre of the plasma, positive when the surface lies towards the edge of the plasma, and should pass through zero when the critical surface lies at $r_s = 0.746\,a$. This is exactly the behaviour exhibited in Fig. 5. The torque passes through zero when the radius of the critical surface is slightly greater than $0.746\,a$ because of the residual influence of the torque exerted in the edge boundary layer. As the velocity shear parameter α_1 is gradually decreased the zero torque point moves outwards in r_s until it approaches the edge of the plasma. This is exactly the behaviour predicted by analytic theory as the edge torque becomes gradually more significant with respect to the torque exerted at the critical surface. Figure 6 shows the normalized torque $\hat{T}$ exerted on the plasma plotted as a function of the angular velocity parameter z for various values of the velocity shear parameter α_1. It can been seen that the torque versus angular velocity curve for a plasma with non-zero angular velocity shear exhibits the same basic features as that for a rigidly rotating plasma, except that the former curve tends to be more strongly peaked than the latter. The two curves merge smoothly in the limit $\alpha_1 \to 0$.

In summary, a code has been developed in order to directly evaluate the torque exerted on the plasma in the presence of finite velocity shear. The results of the code agree with analytic theory in both the strong ($\alpha_1 \gg 1$) and zero ($\alpha_1 = 0$) shear limits. In the strong shear limit the analytic result corresponds to a standard result in hydrodynamic theory. The behaviour of the torque in the weak shear limit is directly analogous to that exhibited in the strong shear limit. Moreover, the torque versus angular velocity curve evolves quite smoothly from that characteristic of the zero shear limit to that characteristic of the strong shear limit as the velocity shear in the plasma is gradually increased from zero. The results of the code strongly support the view that the rather counter-intuitive sign of the torque found in the preceding analysis is, in fact, the correct sign for the system under investigation.

III Summary

In this paper the response of a single component plasma confined in a Penning-Malmberg trap to an oscillating, non-axisymmetric, electric field is calculated using a phenomenological fluid model. The main advantage of this approach is that the experimentally determined values of the radial angular momentum transport and the drag torque due to magnetic field asymmetries can be incorporated into the analysis. At present, these two effects are not well understood on a microscopic level.

A single component plasma confined in a Penning-Malmberg trap generally satisfies the inequality

$$|\Omega_\theta| \gg \gamma_\nu \gg \gamma_d, \tag{131}$$

where Ω_θ is the angular rotation velocity of the plasma, γ_ν is the rate at which viscosity relaxes the angular velocity profile across the whole plasma cross-section, and γ_d is the rate at which angular momentum is lost from the plasma as a consequence of magnetic field asymmetries. Clearly, the time scale on which the plasma spins down, or spins up, under the influence of the drag torque, or any external torque (assuming that the latter is of the same order of magnitude as the former, which it ultimately balances), is much longer than the time scale on which the plasma angular velocity profile relaxes to that of a rigid rotator. It is, therefore, legitimate to calculate the external torque assuming that the angular velocity profile is close to that of a rigid rotator.

The non-linear torque exerted on a rigidly rotating plasma by an oscillating, non-axisymmetric electric field is a highly non-monotonic function of the plasma angular velocity. The torque *vs.* angular velocity curve is dominated by a series of *sharp resonances* at which the angular phase velocity of a particular poloidal harmonic of the external field matches the angular rotation velocity of the plasma. The resonance condition for the mth harmonic is

$$\Omega_\theta = \frac{\Omega}{m}, \tag{132}$$

where Ω is the oscillation frequency of the external field. In practice, there are many resonances since the external electric field is usually generated by voltages applied to conducting plates and is, therefore, not a pure poloidal harmonic.

The width of each resonance (in units of angular velocity) is of order γ_ν; *i.e.*, it is extremely small compared to the angular velocity of the plasma. Close to the centre of the resonance (*i.e.*, $|\Omega_\theta - \Omega/m| \ll \gamma_\nu$) the net torque exerted on the plasma increases linearly with the difference in phase velocity between the plasma and the resonant component of the electric field (*i.e.*, with $\Omega_\theta - \Omega/m$). In this limit, the torque is fairly evenly distributed throughout the plasma. Far from the centre of the resonance (*i.e.*, $|\Omega_\theta - \Omega/m| \gg \gamma_\nu$) the net torque exerted on the plasma decreases like one over the square root of the difference in phase velocity. In this limit, the torque is exerted in a narrow edge layer of thickness $\sqrt{\gamma_\nu/|\Omega_\theta - \Omega/m|}$ relative to the plasma minor radius. The maximum torque exerted on the plasma is *independent* of the viscosity, and varies as the square of the amplitude of the external perturbation. The net torque exerted on the plasma by the mth poloidal harmonic of the external electric field is *negative* when the field rotates *faster* than the plasma (*i.e.*, when $\Omega/m > \Omega_\theta$), and *positive* when the field rotates *slower* than the plasma. Thus, the torque is such as to push the plasma angular velocity away from its resonant value Ω/m.

In the presence of a small amount of angular velocity shear the picture outlined above is modified somewhat. If the resonance condition $\Omega_\theta(r) = \Omega/m$ *is not* satisfied inside the plasma then the torque is exerted in a narrow edge layer, as described above. However, if the resonance condition *is* satisfied inside the plasma then the dominant torque is exerted in a narrow layer centred on the critical surface, $\Omega_\theta(r_s) = \Omega/m$. The thickness of the critical layer is of order $(\gamma_\nu/\Delta\Omega_\theta)^{1/3}$ relative to the minor radius of the plasma, where $\Delta\Omega_\theta$ is a measure of the angular velocity shear. The amplitude of the torque exerted on a critical layer is comparable to the peak torque exerted on a rigidly rotating plasma. The sign of the torque is such that when most of the plasma is spinning faster than the external perturbation the torque is positive, and *vice versa*. In other words, the sign of the torque is completely compatible with that found in the absence of angular velocity shear. The sign of the torque exerted on a critical surface is determined by a standard result in hydrodynamic theory. Namely, the torque exerted on a critical surface always acts in the same direction as the local viscous torque. This ensures that velocity shear driven plasma instabilities always act to relax the plasma angular velocity profile back to that of a rigid rotator; *i.e.*, they reduce the source of free energy which drives them unstable, in accordance with d'Alembert's principle. As the plasma angular velocity shear gradually decays

under the action of viscosity the torque exerted on the plasma as a function of its average angular rotation velocity asymptotes smoothly to that calculated in the limit of zero angular velocity shear.

It is only possible to form a stable balance point between the torque exerted on the plasma by the mth poloidal harmonic of the external electric field and the drag torque due to asymmetries in the magnetic field if the plasma angular rotation velocity is close to, but slightly larger than, the resonant velocity Ω/m. There is a critical amplitude of the mth harmonic below which the balance point is suddenly lost. At the critical amplitude the balance point lies on that peak of the torque *vs.* angular velocity curve which occurs in the immediate vicinity of $\Omega_\theta = \Omega/m$. The critical amplitude depends on the drag rate γ_d, but is independent of the plasma viscosity. After the balance point is lost the plasma spins down under the influence of the drag torque. The plasma either comes into equilibrium with a higher mode number harmonic of the external field (at a lower angular rotation velocity), or spins down until the edge of the plasma hits the electrodes and confinement is lost. Note that this process is *irreversible*; *i.e.*, the balance point with the mth harmonic cannot be restored by simply raising the amplitude of the mth harmonic above its critical value again.

The somewhat surprising sign of the torque obtained in this paper (*i.e.*, such that the torque is positive when the external perturbation rotates slower than the plasma, and *vice versa*) is not observed experimentally. The most likely explanation for this is that the experimental torque, which has the opposite sign, is predominately determined by a different mechanism to that discussed above. Indeed, there is some evidence, mainly from pure ion experiments, that the torque is somehow related to the dynamics of particles along the axis of the trap. For instance, it is found that the momentum injection is most effective when the externally applied electric field varies strongly along the axis of the trap.[23] Furthermore, in pure ion experiments the 'slip frequency' (*i.e.*, the difference between the rotation frequency of the externally applied perturbation and the angular rotation frequency of the plasma) is found to be closely correlated with ion bounce frequency between the two ends of the trap.[24] Axial dynamics are not taken into account in this paper, which only considers infinitely long traps in which there is no axial variation. It may be that, in practice, torques arising from axial dynamics (*e.g.*, the torque associated with the 'rotational pumping' mechanism discussed

by Crooks and O'Neil[25]) dominate the torque arising from the mechanism described in this paper. Another possibility is that it is simply not appropriate to treat a plasma confined in a Penning-Malmberg trap as a fluid, as is attempted in the above. Furthermore, the conventional expression for the viscosity operator adopted in this paper may turn out to differ quite substantially from the actual (and, as yet, unknown) viscosity operator. On a more optimistic note, there is some *indirect* evidence that, under certain circumstances, a non-axisymmetric external perturbation which rotates more slowly than the plasma can increase the plasma angular momentum. Notte and Fajans[26] find that small, static, non-axisymmetric, externally applied electric fields can increase the lifetime of an electron plasma confined in a Penning-Malmberg trap, whereas large fields decrease the lifetime of the plasma. The conventional explanation of this effect is that the applied perturbation cancels the intrinsic asymmetry in the equilibrium radial electric field of the trap. However, as pointed out by Notte and Fajans, in this case the size of the applied perturbations would correspond to an implausibly large intrinsic asymmetry. Perhaps the mechanism outlined in this paper is relevant to this situation?

Acknowledgments

The author would like to thank F. Anderegg, C.F. Driscoll, X.-P. Huang, and T.M. O'Neil, of the University of California at San Diego for helpful discussions during the preparation of this paper.

This research was funded by the U.S. Department of Energy under contract No. DE-FG05-96ER-54346.

References

[1] R.C. Davidson, *Physics of nonneutral plasmas*, (Addison-Wesley, Redwood City, CA, 1990).

[2] T.B. Mitchell, C.F. Driscoll, and K.S. Fine, Phys. Rev. Lett. **71**, 1371 (1993).

[3] X.-P. Huang, and C.F. Driscoll, Phys. Rev. Lett. **72**, 2187 (1994).

[4] T.B. Mitchell, and C.F. Driscoll, Phys. Rev. Lett. **73**, 2196 (1994).

[5] B.P. Cluggish, and C.F. Driscoll, Phys. Rev. Lett. **74**, 4213 (1995).

[6] X.-P. Huang, K.S. Fine, and C.F. Driscoll, Phys. Rev. Lett. **74**, 4424 (1995).

[7] T.M. O'Neil, Comments Plasma Phys. Cont. Fusion **5**, 231 (1980).

[8] X.-P. Huang, F. Anderegg, T.M. O'Neil, C.F. Driscoll, and E.M. Hollmann, Bull. Amer. Phys. Soc. **40**, 1740 (1995).

[9] C.F. Driscoll, J.H. Malmberg, and K.S. Fine, Phys. Rev. Lett. **60**, 1290 (1988).

[10] S.I. Braginskii, in *Reviews of modern physics* (ed. M.A. Leontovich), (Consultants Bureau, New York, 1965), Vol. 1.

[11] K. Brau, M. Bitter, R.J. Goldston, D. Manos, K. McGuire, and S. Suckewer, Nucl. Fusion **23**, (1983).

[12] T.M. O'Neil, and C.F. Driscoll, Phys. Fluids **22**, 266 (1979).

[13] T.M. O'Neil, Phys. Rev. Lett. **55**, 943 (1985).

[14] C.F. Driscoll, Bull. Amer. Phys. Soc. **40**, 1746 (1995).

[15] C.F. Driscoll, and J.H. Malmberg, Phys. Rev. Lett. **50**, 167 (1983).

[16] T.H. Stix, Phys. Fluids **16**, 1260 (1973).

[17] C.F. Driscoll, K.S. Fine, and J.H. Malmberg, Phys. Fluids **29**, 2015 (1986).

[18] L. Brillouin, Phys. Rev. **67**, 260 (1945).

[19] R. Fitzpatrick, in *Theory of fusion plasmas* (eds. E. Sindoni and J. Vaclavik), Proceedings of the Joint Varenna-Lausanne International Workshop, Varenna 1992 (Società Italiana di Fisica, Bologna, 1992), p. 147.

[20] R.H. Levy, Phys. Fluids **8**, 1288 (1965).

[21] S.A. Maslowe, in *Hydrodynamic instabilities and the transition to turbulence* (eds. H.L. Swinney, and J.P. Gollub), (Springer-Verlag, Berlin, 1981), p. 181.

[22] J.R. Foote, and C.C. Lin, Quart. Appl. Math. **8**, 265 (1950).

[23] C.F. Driscoll, private communication (1996).

[24] E.M. Hollmann, X.-P. Huang, F. Anderegg, C.F. Driscoll, T.M. O'Neil, Bull. Am. Phys. Soc. **41**, 1605 (1996).

[25] S.M. Crooks, and T.M. O'Neil, Phys. Plasmas **2**, 355 (1995).

[26] J. Notte, and J. Fajans, Phys. Plasmas **1**, 1123 (1994).

A Layer physics

In the immediate vicinity of the critical surface Eq. (102) reduces to

$$x\,\frac{d^2\tilde{\psi}}{dx^2}-\lambda_s\tilde{\psi}\simeq-\mathrm{i}\,\sigma_s\mu_s\frac{d^4\tilde{\psi}}{dx^4}+\mathrm{i}\,\sigma_s\kappa_s\frac{d^2\tilde{\psi}}{dx^2},\tag{A1}$$

where

$$\sigma_s = \mathrm{sgn}(m)\,\mathrm{sgn}(\Omega'_\theta(r_s)\,),\tag{A2a}$$

$$\mu_s = \frac{\nu}{|m|\,\kappa\,(r\,|\Omega'_\theta|)_{r_s}\,{r_s}^2},\tag{A2b}$$

$$\kappa_s = \frac{\gamma_d}{|m|\,\kappa\,(r\,|\Omega'_\theta|)_{r_s}}.\tag{A2c}$$

It is convenient to define

$$\phi=\frac{d^2\tilde{\psi}}{dx^2}.\tag{A3}$$

Let $\phi(x)=\phi_e(x)+\phi_o(x)$, where $\phi_e(-x)=\phi_e(x)$ and $\phi_o(-x)=-\phi_o(x)$. Equation (A.1) can be re-expressed as a pair of symmetrized equations:

$$\frac{d^2(x\,\phi_o)}{dx^2}-\lambda_s\,\phi_e = -\mathrm{i}\,\sigma_s\mu_s\,\frac{d^4\phi_e}{dx^4}+\mathrm{i}\,\sigma_s\kappa_s\,\frac{d^2\phi_e}{dx^2}\tag{A4a}$$

$$\frac{d^2(x\,\phi_e)}{dx^2}-\lambda_s\,\phi_o = -\mathrm{i}\,\sigma_s\mu_s\,\frac{d^4\phi_o}{dx^4}+\mathrm{i}\,\sigma_s\kappa_s\,\frac{d^2\phi_o}{dx^2}.\tag{A4b}$$

Let

$$\phi_{e,o}(x)=\int_{-\infty}^{+\infty}\bar{\phi}_{e,o}(p)\,e^{\mathrm{i}\,px/\mu_s^{1/3}}\,dp,\tag{A5}$$

where $\bar{\phi}_e(-p)=\bar{\phi}_e(p)$ and $\bar{\phi}_o(-p)=-\bar{\phi}_o(p)$. Equations (A.4) transform to

$$\frac{d\bar{\phi}_o}{dt} = \sigma_s\,\bar{\phi}_e,\tag{A6a}$$

$$\frac{d\bar{\phi}_e}{dt} = \sigma_s\,\bar{\phi}_o,\tag{A6b}$$

where

$$t = -\mathrm{i}\,\frac{\sigma_s\lambda_s{\mu_s}^{1/3}}{p} + \frac{\kappa_s}{{\mu_s}^{1/3}}\,p + \frac{p^3}{3}. \tag{A7}$$

The square integrable solutions to Eqs. (A.6) are

$$\bar{\phi}_o(t) = B\,\mathrm{e}^{-t}, \tag{A8a}$$

$$\bar{\phi}_e(t) = -\sigma_s B\,\mathrm{e}^{-t} \tag{A8b}$$

for $t > 0$.

The layer solution must be asymptotically matched to the solution of the diocotron equation in the region ${\mu_s}^{1/3} \ll |x| \ll 1$, which is equivalent to the region ${\mu_s}^{1/3} \ll |p| \ll 1$. The asymptotic behaviour of the Fourier transformed layer solutions in the matching region is

$$\bar{\phi}_o(p) \simeq B\left(\mathrm{i}\,\frac{\sigma_s\lambda_s{\mu_s}^{1/3}}{p} + 1 + O(p)\right), \tag{A9a}$$

$$\bar{\phi}_e(p) \simeq -\sigma_s B\left(\mathrm{i}\,\frac{\sigma_s\lambda_s{\mu_s}^{1/3}}{p} + 1 + O(p)\right) \tag{A9b}$$

for $p > 0$. The asymptotic behaviour in real space is

$$\phi_o(x) \simeq 2\mathrm{i}\,B\,{\mu_s}^{1/3}\left(\frac{1}{x} + \mathrm{i}\,\frac{\pi\sigma_s\lambda_s}{2} + O(x)\right), \tag{A10a}$$

$$\phi_e(x) \simeq 2\mathrm{i}\,B\,{\mu_s}^{1/3}\left(\,\mathrm{i}\,\pi\sigma_s\,\delta(x) + \lambda_s\ln x + C' + O(x)\,\right) \tag{A10b}$$

where $x > 0$ and C' is some constant.

According to Eqs. (107), (109), and (A.1), the asymptotic behaviour of the solution to the diocotron equation in the vicinity of the critical surface is

$$\phi_o(x) \simeq \frac{\lambda_s\tilde{\psi}_e(x)}{x} = \lambda_s\Psi_s\left(\frac{1}{x} + \frac{\Delta_s}{2} + O(x)\right), \tag{A11a}$$

$$\phi_e(x) \simeq \frac{\lambda_s\tilde{\psi}_o(x)}{x} = \lambda_s\Psi_s\left(\lambda_s(\ln x - 1) + \frac{C}{2} + O(x)\right), \tag{A11b}$$

where $C = (\Psi'_{s+} + \Psi'_{s-})/\Psi_s$ and $x > 0$. It follows from Eqs. (A.10) and (A.11) that

$$B = -\mathrm{i}\,\frac{\lambda_s}{2{\mu_s}^{1/3}}\,\Psi_s, \tag{A12}$$

and

$$\Delta_s = \mathrm{i}\,\pi\sigma_s\lambda_s. \tag{A13}$$

Table captions

Table I: The first few roots of Eq. (55)

Table II: The first five roots of Eq. (65)

Table III: g_m and $T_m(\max)$, evaluated for various values of m

Figure captions

Fig. 1: Schematic diagram of the variation of the torque function T_m with the plasma angular velocity Ω_θ

Fig. 2: Schematic diagram showing how the steady state angular velocity of the plasma is determined by the crossing points of the electromagnetic torque curve and the drag torque curve

Fig. 3: The function $t_m(r/a)$ calculated for $m = 2$, $\gamma_d \ll \gamma_\nu$, and various values of $\zeta = \kappa(\Omega_\theta - \Omega/m)/(g_m \gamma_\nu)$. The solid curve corresponds to $\zeta = 100$, the dotted curve to $\zeta = 10$, the the dashed curve to $\zeta = 1$, the dot short-dash curve to $\zeta = \sqrt{0.1}$, and the dot long-dash curve to $\zeta = 0.1$.

Fig. 4: The normalized torque density $\hat{t}(r/a)$ calculated for $m = 2$, $\alpha_1 = 10^4$, and $z = -500$. The radius of the critical surface ($r_s = 0.666\,a$) is indicated by a vertical dashed line.

Fig. 5: The normalized torque $\hat{T}$ plotted as a function of the radius of the critical surface r_s for $m = 2$ and $\alpha_1 = 2000$. The radius at which the torque is supposed to reverse sign according to $\alpha_1 \gg 1$ analytic theory ($r_s = 0.746\,a$) is indicated by a vertical dashed line.

Fig. 6: The normalized torque $\hat{T}$ plotted as a function of the angular velocity parameter z for $m = 2$ and various values of the velocity shear parameter α_1. The long-dash curve corresponds to $\alpha_1 = 0$, the short-dash curve to $\alpha_1 = 100$, the dotted curve to $\alpha_1 = 200$, the solid curve to $\alpha_1 = 300$, and the dot-dash curve to $\alpha_1 = 400$.

m	1st root	2nd root	3rd root
1	3.05	6.71	9.97
2	4.20	8.02	11.35
3	5.32	9.28	12.68

Table I:

No.	$\sqrt{-\beta}$
1	0
2	5.136
3	8.417
4	11.620
5	14.796

Table II:

m	g_m	$T_m(\max)$
2	9.86	0.129
3	10.93	0.190
4	12.32	0.225
5	13.85	0.248
10	22.11	0.297
20	39.23	0.325
30	56.48	0.334

Table III:

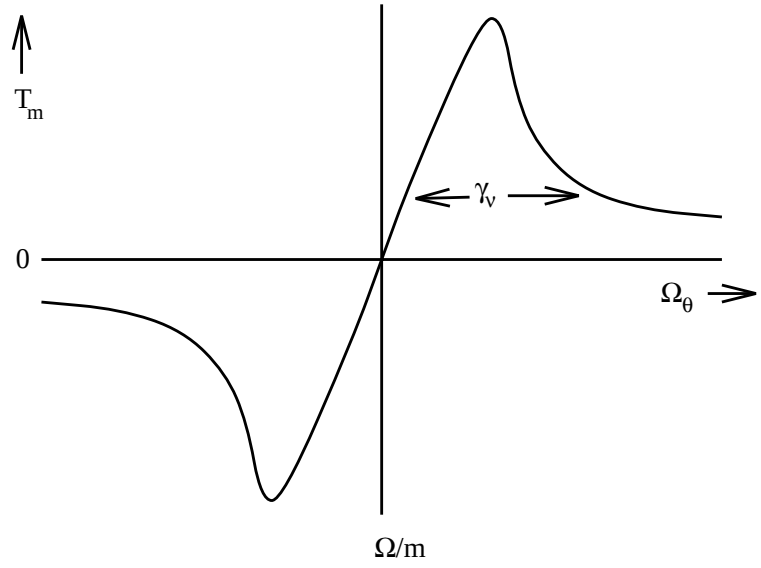

Figure 1:

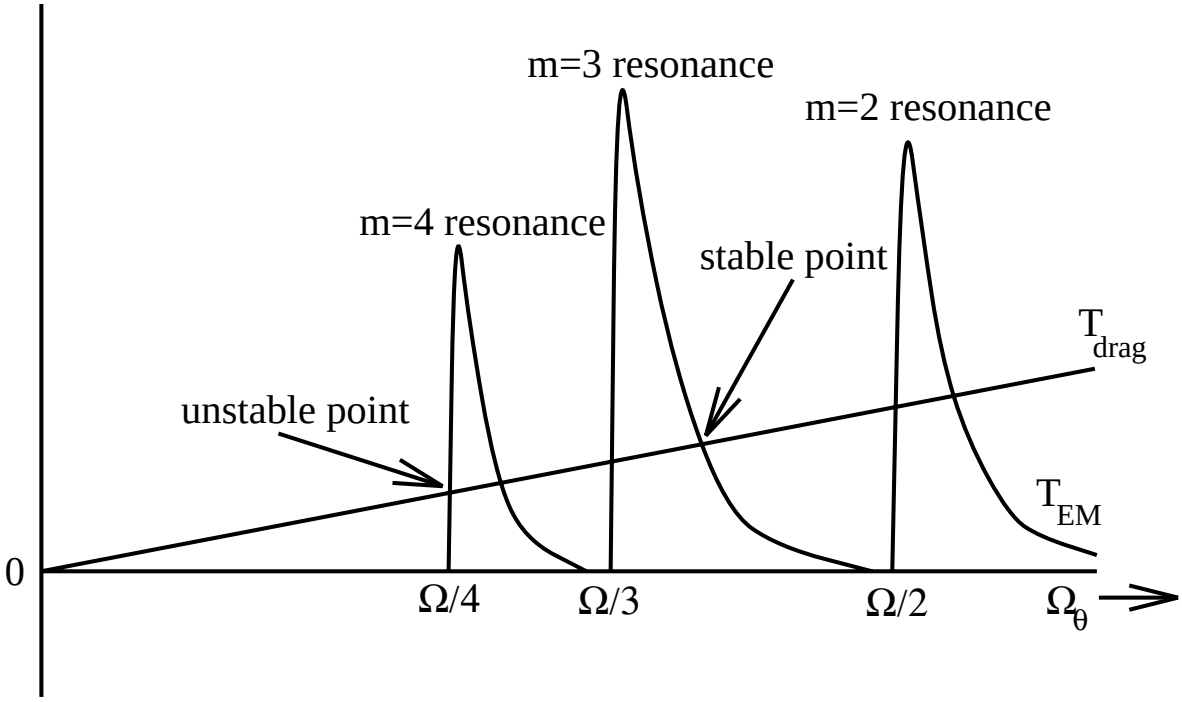

Figure 2:

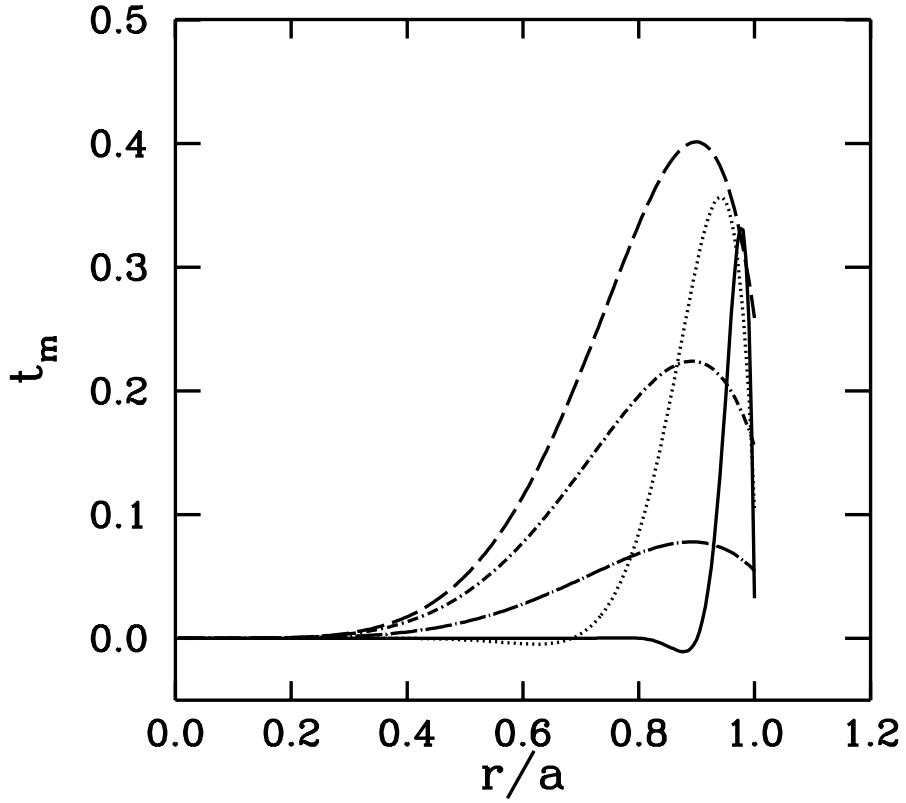

Figure 3:

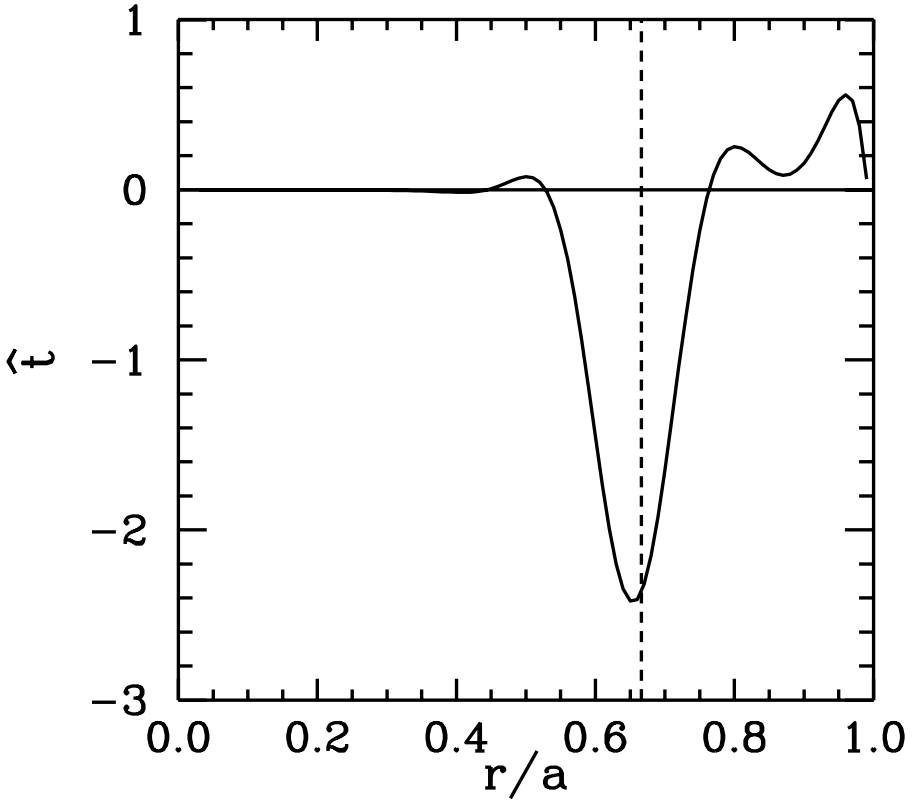

Figure 4:

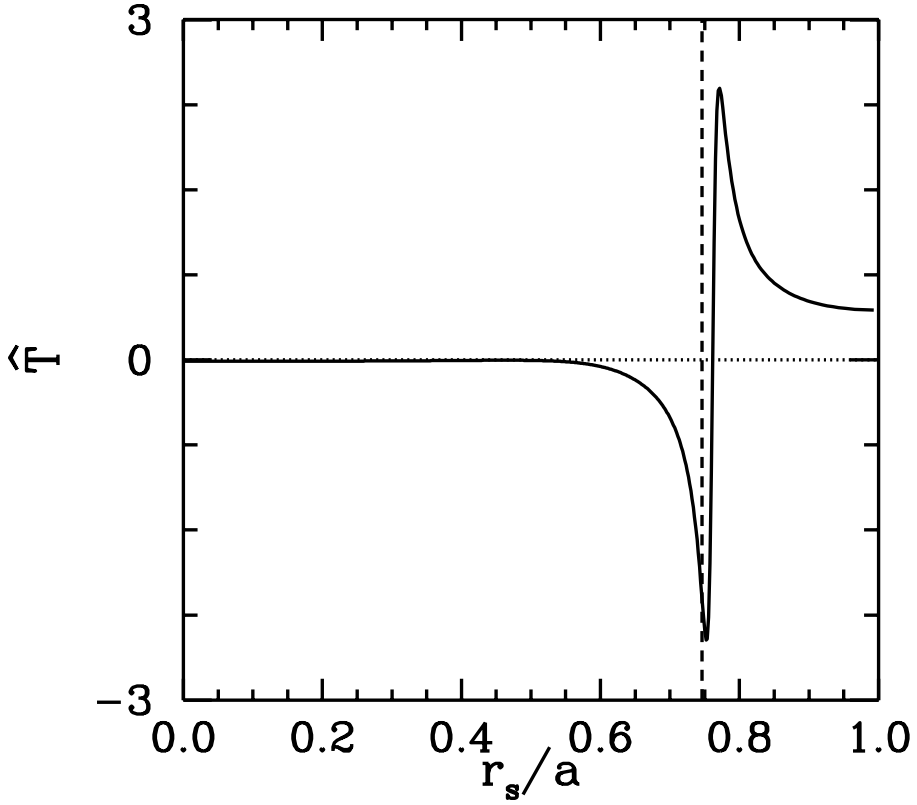

Figure 5:

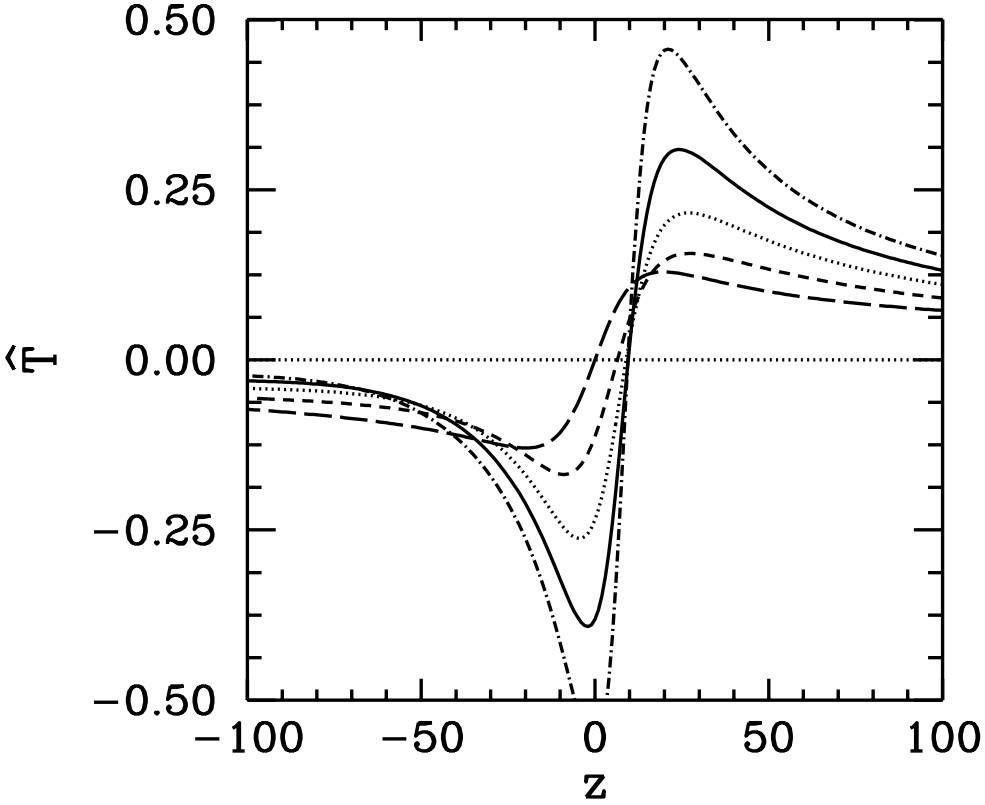

Figure 6: